

Beam-Steering Based on Dispersive Optical Phased Array for FMCW LiDAR Application

Xingyi Jiang¹, Zhaoyang Zhang¹, Qikai Huang¹, Qiang Zhang², Jianyi Yang¹, Hui Yu^{2*}

¹College of Information Science and Electronic Engineering, Zhejiang University, Hangzhou 310027, China

²Zhejiang Lab, Hangzhou 311121, China

*Corresponding author: huiyu@zhejianglab.com

Abstract: We demonstrate dispersive optical phased arrays based on the Si₃N₄-on-Si platform. Two-dimensional beam steering across a 45.6° × 10° FOV with a beam width of 1.45° × 0.032° is achieved by wavelength tuning alone. Besides, FMCW ranging operation at a target distance of 10 m are experimentally performed. © 2023 The Author(s)

1. Introduction

Over the past few decades, optical phased arrays (OPAs) have demonstrated significant benefits including all solid-state configurations, compact size, and low cost [1-6]. Most OPAs in previous work realized beam steering based on massive phase shifter arrays, which led to complicated control and high power consumption. Dispersive OPAs based on the delay line waveguide may provide another solution to address these problems [7-10].

The principle of operation of OPAs and arrayed waveguide gratings (AWGs) is basically the same, despite that the interference region of OPA is free space, while beams in AWG interfere in the star coupler. The phase difference between adjacent antennas in OPA is obtained by tuning the working wavelength alone, thanks to the array waveguides with a fixed optical path difference ΔL . Consequently, continuous beam steering in the phase-array direction is achieved. Since beams will be steered periodically in the phase-array direction, the wavelength range between two adjacent overlapping beams is called the free spectral range (FSR). Moreover, the diffraction of the grating antenna enables beam scanning in the orthogonal dimension.

In this work, we design and demonstrate three 32-channel dispersive OPAs with FSRs of ~ 7 nm, ~ 10 nm and ~ 18 nm. To improve the resolution in the grating direction, an optimized Si₃N₄-assisted grating antenna is used to decrease the emission rate as well as the beam divergency. By tuning the wavelength, the output beam is steered across the FOV of 45.6° × 10° with a beam divergence of 1.45° × 0.032°. Furthermore, a ranging distance of 10 m is achieved by combining the frequency-modulated continuous wave (FMCW) with the dispersive OPA.

2. Device Architecture

Three OPAs with path length difference ΔL of 58.08 μm , 86.308 μm and 192 μm , corresponding to FSRs of ~ 18 nm, ~ 10 nm, ~ 7nm, are shown in Fig. 1. Light is coupled into the chip through a grating coupler, and a five-layer splitter tree using silicon 1×2 multi-mode interferometers (MMIs) distributes the beam equally into 32 separate channels. Phase differences are introduced after beam transmission through the silicon arrayed waveguides. Moreover, thermal-optical (TO) phase shifters are integrated to perform one-time phase calibration against the phase errors due to fabrication imperfections. Finally, a 3 mm-long grating antenna array with a pitch of 2 μm radiates the light into free space. A scanning electron microscope (SEM) image of the Si₃N₄-on-Si grating antenna with a low emission rate of nearly 15 dB/cm [11] is shown in the inset of Fig. 1. A 30 nm Si₃N₄ film is deposited above the 220 nm silicon with an oxide gap of 40 nm. Next, the thin nitride layer is etched to form the grating groves, and the period and duty cycle of the grating are 610 nm and 41.8%, respectively.

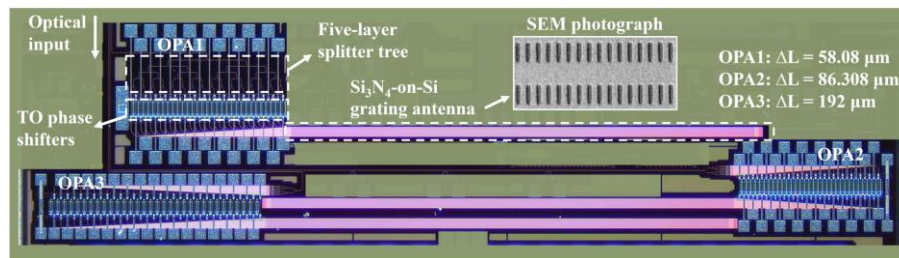


Fig. 1. Microscope photograph of the fabricated 32-channel dispersive OPAs with the path length differences ΔL of 58.08 μm , 86.308 μm and 192 μm . And the inset is the scanning electron micrograph (SEM) of the Si₃N₄-on-Si grating antenna.

3. Beam Steering and FMCW Ranging Operation

We tested beam steering characteristics of three 32-channel dispersive OPAs. The power consumptions of initial phase calibration for three devices OPA1-3 are 190 mW, 40 mW and 0 mW, respectively. The steering efficiency of OPA1 and OPA2 in the phased-array direction is $2.5^\circ/\text{nm}$ and $4.5^\circ/\text{nm}$, as shown in Fig. 2(a) and Fig. 2(b). A much higher steering efficiency of $6.4^\circ/\text{nm}$ is measured in OPA3, which is shown in Fig. 2(c). Fig. 2(d) describes that two-dimensional beam steering across a FOV of $45.6^\circ \times 10^\circ$ is achieved by tuning the wavelength from 1500 nm to 1575 nm with a step of 0.3 nm. From Fig. 2(e), the full-width at half-magnitude (FWHM) beam divergence is measured to be $1.45^\circ \times 0.032^\circ$.

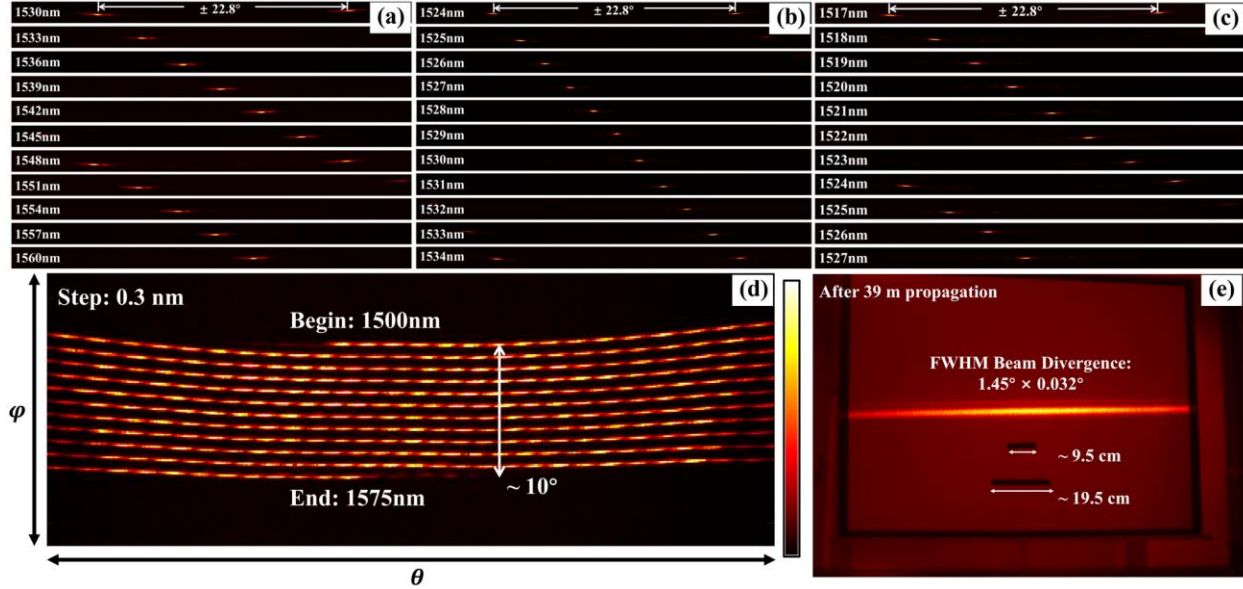


Fig. 2. Measured far-field patterns, two-dimensional beam steering with (a) FSR of ~ 18 nm; (b) FSR of ~ 10 nm; (c) FSR of ~ 7 nm. (d) Two-dimensional beam steering pattern with wavelength tuning from 1500 nm to 1575 nm observed on the screen. (e) The beam profile after 39 m propagation.

The dispersive OPA with the FSR of ~ 7 nm is integrated into a FMCW ranging system, and the experimental setup is depicted in Fig. 3(a). The triangular chirp FMCW signal (6 GHz \sim 9 GHz) is generated from a PLL-based synthesizer. The chirp period is 1 ms. A lithium niobate in-phase/quadrature (IQ) modulator is used to upconvert the chirp to the optical region. Then, the light is amplified by an erbium-doped fiber amplifier (EDFA) and distributed by a 1/99 optical power splitter: the 1% power as the local oscillator (LO) light is routed to a 50/50 power splitter, and the 99% power is fed into the OPA chip. The backscattered light from the target is collected by a fiber collimator (Thorlabs F810APC-1550) and mixed with LO. Subsequently, the beat frequency corresponding to the ranging distance is produced by a balanced amplified detector. Finally, the electrical signal is fed to an oscilloscope (Keysight DSOX3054T) for record and real-time FFT analysis. In the experiment, the optical power fed into the OPA chip is 12.4 dBm and the power of the main lobe is -7 dBm.

The beat signals in the time domain and the frequency domain with a target distance of 10 m are shown in Fig. 3(b) and Fig. 3(c), respectively. And the beat frequency is 695 kHz and the signal-to-noise ratio (SNR) is ~ 36.8 dB. Figure 2(d) shows the measured beat frequency with the distance of the target varying from 2.46 m to 10 m. It shows a good linear correlation between the beat frequency and target distance, and the slope of the linear fit is 39.97 kHz/m, which is in line with the chirp slope of 6 THz/s.

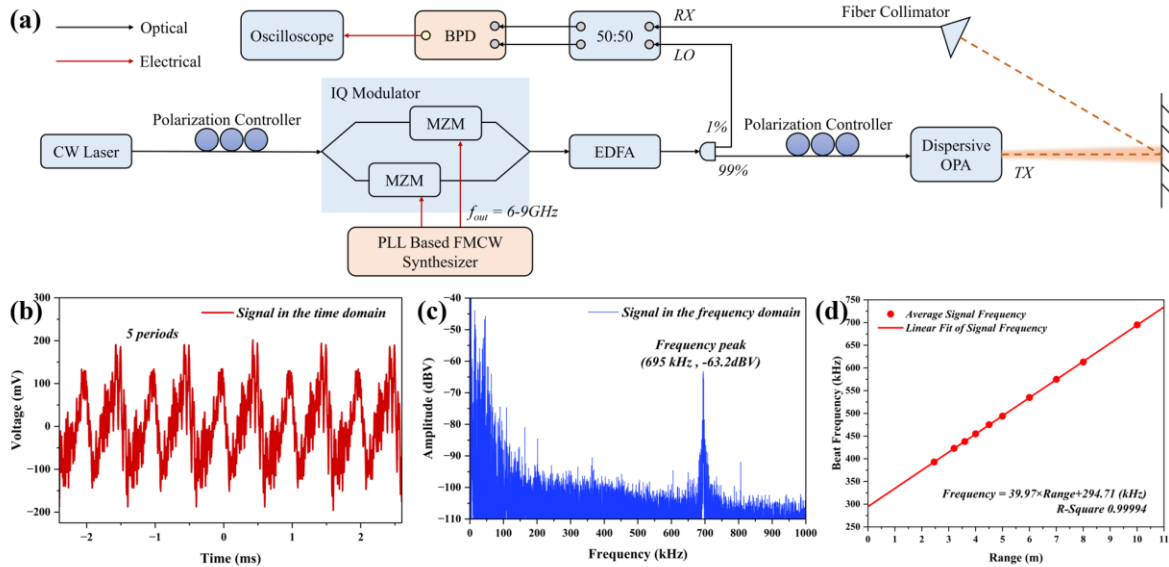


Fig. 3. (a) Experimental setup of ranging operation using the dispersive OPA with FSR of ~ 7 nm and PLL-based FMCW synthesizer. CW: Continuous wave; MZM: Mach-Zehnder modulator; EDFA: erbium-doped fiber amplifier; BPD: balanced photodetector. (b) and (c) are the time domain and frequency domain signals corresponding to the target of 10 m, respectively. (d) Measured the beat frequency with different ranging distance and linear fit of the frequency.

4. Conclusion

We experimentally demonstrate beam scanners based on three types of dispersive OPAs with ~ 7 nm, ~ 10 nm and ~ 18 nm FSR. Two-dimensional beam steering with a measured FOV of $45.6^\circ \times 10^\circ$ is achieved by tuning the wavelength from 1500 nm to 1575 nm. The beam divergence is measured to be $1.45^\circ \times 0.032^\circ$. Furthermore, FMCW ranging operation up to 10 m is also presented by using the dispersive OPA. The proposed beam scanner offers compact size, simplified control, low power consumption, high resolution and allows massively parallel beam steering by WDM multiplexing, which offers a flexible and promising solution to applications including LiDAR, free-space optical communication.

Acknowledgement

The authors would like to thank Dr. Bing Wei, Training Platform of Information and Microelectronic Engineering in Polytechnic Institute of Zhejiang University.

References

- [1]. M. J. Heck, et al. "Highly integrated optical phased arrays: photonic integrated circuits for optical beam shaping and beam steering", *Nanophotonics* **6**(1), 93-107 (2017).
- [2]. Poulton, C. V., et al. "Long-range lidar and free-space data communication with high-performance optical phased arrays", *IEEE Journal of Selected Topics in Quantum Electronics* **25**(5), 1-8 (2019).
- [3]. Kang, G., et al. "Silicon-based optical phased array using electro-optic p-i-n phase shifters", *IEEE Photonics Technology Letters* **31**(21), 1685-1688 (2019).
- [4]. J. Guglielmon, et al., "Optical Phased Array Super-Cell Beyond the Reticle Limit", 2023 Conference on Lasers and Electro-Optics (CLEO), San Jose, CA, USA, 2023, pp. 1-2.
- [5]. S. A. Miller, et al., "512-Element Actively Steered Silicon Phased Array for Low-Power LIDAR", Conference on Lasers and Electro-Optics, OSA Technical Digest (online) (Optica Publishing Group, 2018), paper JTh5C.2.
- [6]. W. Xu, et al., "Fully Integrated Solid-State LiDAR Transmitter on a Multi-Layer Silicon-Nitride-on-Silicon Photonic Platform", *Journal of Lightwave Technology* **41**(3), 832-840 (2023).
- [7]. Van Acoleyen, et al. "Two-dimensional dispersive off-chip beam scanner fabricated on silicon-on-insulator", *IEEE Photonics Technology Letters* **23**(17), 1270-1272 (2011).
- [8]. Bogaerts, W., et al. "A 2d pixelated optical beam scanner controlled by the laser wavelength", *IEEE Journal of Selected Topics in Quantum Electronics* **27**(1), 1-12 (2021).
- [9]. Munoz, P., et al. "Scalable switched slab coupler based optical phased array on silicon nitride", *IEEE Journal of Selected Topics in Quantum Electronics* **28**(5), 1-16 (2022).
- [10]. Y. Misugi, et al. "Low Power Consumption 2D Beam Scanner Integrated with Wavelength Tunable Laser Diode", 2022 European Conference on Optical Communication (ECOC), Basel, Switzerland, 2022, pp. 1-4.
- [11]. Zhaoyang Zhang, et al. "A Tri-Layer Si₃N₄-on-Si Optical Phased Array With High Angular Resolution", *IEEE Photonics Technology Letters*, **34**(20), 1108-1111 (2022).